Ritual revealed: psychotropic substances in a Ptolemaic Egyptian vase

Davide Tanasi
University of South Florida

Branko van Oppen de Ruiter
Tampa Museum of Art

Fiorella Florian
University of Trieste

Radmila Pavlovic
University of Milan

Luca Chiesa
University of Milan

Igor Fochi
Thermo Fischer Scientific

Chiaramaria Stani
CERIC-ERIC

Lisa Vaccari
Elettra - Sincrotrone Trieste

Dale Chaput
University of South Florida

Giorgio Samorini
Indipendent researcher

Alberto Pallavicini
https://orcid.org/0000-0001-7174-4603

Anastasia Gaetano
University of Trieste

Sabina Licen
University of Trieste

Pierluigi Barbieri
University of Trieste

Enrico Greco (✉ enrico.greco@units.it)
University of Trieste   https://orcid.org/0000-0003-1564-4661

Physical Sciences - Article

Abstract

This study presents a comprehensive multimodal analytical study of an Egyptian ritual Bes-vase, of the 2nd century BCE employing cutting-edge proteomics, metabolomics, genetics techniques, and synchrotron radiation-based Fourier Transformed Infrared microSpectroscopy (SR μ-FTIR) to characterize organic residues of its content. We successfully identified the presence of various nutraceutical, psychotropic, medicinal, and biological substances, shedding light on the diverse components of a liquid concoction used for ritual practices in Ptolemaic Egypt. Using LC-MS/MS with a new methodological approach, we identified key proteins and metabolites, enabling the identification of botanical sources, confirmed by genetic sequences. Our analyses revealed traces of *Peganum harmala*, *Nimphaea nouchali var. caerulea*, and a plant of the Cleome genus, all of which are traditionally proven to have psychotropic and medicinal properties. Additionally, the identification of human fluids suggests their direct involvement in these rituals. Furthermore, metabolomics and SR μ-FTIR analyses also revealed the presence of fermented fruit-based liquid and other ingredients such as honey or royal jelly. The identification of specific chemical compounds, such as alkaloids and flavonoids, provides insight into the psychoactive and therapeutic uses of these in ancient ritual practices. This multidisciplinary study highlights the complexity of ancient cultures and their interactions with psychoactive, medicinal, and nutraceutical substances. These findings contribute to our understanding of ancient belief systems, cultural practices, and the utilization of natural resources, ultimately enhancing our knowledge of past societies and their connection to the natural world.

Summary

The investigation into origins and meaning of ancient religious rituals is a central research topic in archaeology and anthropology. Today, we possess a wealth of well-preserved artifacts, often in their original form, that serve as compelling narratives from both cultural and material perspectives. Through the application of integrated analytical techniques and the development of customized methodologies, we have gained the ability to decipher and extract biomolecular evidence from the organic residues of those natural substances employed for ritualistic or medicinal purposes within the intricate religious and cultural frameworks of ancient Egyptian civilization.

Introduction

Religion is one of the most fascinating and puzzling aspect of any ancient civilization. In the Mediterranean region no other religion has ever reached the ritual complexity, both in terms of prescriptions and lore, of that developed and practiced by the ancient Egyptians over the course of three and a half millennia. This facet of the ancient Egyptian culture was an intricate nexus of beliefs, magical practices and medical, alchemic and herbalistic procedures all practiced conforming to the events and acts described in their sacred texts. A ritual performance assisted by artificial aids, that in certain specific cults gets to assume a central role, is that associated with "Bes",one of the most fascinating and wildly popular figures of ancient Egyptian religion. By the time of the Ptolemaic Period (ca. 330-30 BCE), or

somewhat earlier, so-called Bes Chambers were built at the site of Saqqara near the Egyptian capital Memphis (south of Cairo) in which poorly understood rituals were carried out [1,2].

The familiar image of Bes is a composite of anthropomorphic and theriomorphic elements, part dwarfish, part feline [3]. He emerged from the magical realm of the world of demons as a guardian figure, and gradually seems to have obtained a more numinous status until, in the Roman Imperial age, he sporadically acquired divine worship. In terms of his functions, Bes provided protection from danger, while simultaneously averting harm, and being able with his power to prevent evil [4]. In critical circumstances, he was also placating in nature as told in the well-known Myth of the Solar Eye [5], when he stopped the wrath of bloodthirsty goddess Hathor serving her an alcoholic beverage, spiked with a plant-based drug, disguised as blood to a deep forgetting sleep on her [6]. In a more private sphere, he was bringer of joy and had a certain regenerative importance contributing to the fulfillment and happiness of family life in all facets of reproduction, from virility and sexuality, via fertility and fecundity, to childbirth and growth. The protection of life and of the household further encompassed the curative powers of Bes, both in terms of medicinal healing and magical purification.

The cult of Bes and the rites surrounding his complex numinous nature are centered in various categories of ritual objects, maintaining certain typological features with stylistic changes over the course of several centuries. Among those objects, a major role was played by the so-called Bes-vases. Such vases are a category of ceramic vessels decorated with the effigy or the head of Bes, that circulated in Egypt from the New Kingdom (16th – 11th century BCE) to the Hellenistic or Ptolemaic (330 – 30 BCE) and Roman Imperial periods (30 BCE – 476 CE), when the production peaked [7,8]. Though most of the known examples, belonging to museums and private collections, are decontextualized and of unrecorded provenience [6], occasionally Bes-vases have been discovered in a variety of different archaeological contexts in Egypt and in the Near East, from funerary [9, 10, 11] to residential [7] and sacred contexts [4] and over a long period of time. It is significant, however, that no such vessels are known to have been excavated in the only cult place certainly attributed to Bes, namely the Chambers at the Anubieion in Saqqara, where other Bes-related artefacts have been unearthed [12].

This almost ubiquitous presence of the Bes-vases in multiple contexts over a long period of time, combined with the changing persona of the figure and its role in ancient Egyptian beliefs, make it extremely difficult to speculate what the contents or roles of such vessels may have been in these rituals. As the Bes figure was revered as a protective genius, it might be assumed that the liquid drunk from these mugs was considered beneficent. But lack of research has prevented scholars from determining if these Bes mugs were used in everyday domestic settings or funerary purposes, medicinal or cosmetic preparations, magic rituals, or religious ceremonies, for promoting fertility, cure illness or ward off evil. Several hypotheses on the content of the Bes-vases have been formulated based on iconographic or mythological sources. However, few of them have ever been tested for traces of organic material [6]. Scholars mainly speculated about the kinds of liquid they could contain, as sacred water or milk, wine or beer, kohl or perfume, lubricant or a medicinal potions [6], with an alcoholic beverage being considered the

more likely due the close connection of Bes with Hathor, "Lady of Drunkenness" [5], and his role in the myth of the Solar Eye [3,6,13].

Kaiser's study on 23 Bes-vases [6], belonging to five different types from six museums, focused on residues of animal proteins through Crossover Electrophoresis (CIEP) and a subsequent aDNA analysis. Of the 23 vessels sampled, just four yielded positive results. One tested positive for protein and DNA of the species *Bos Taurus*, three other examples tested positive just for DNA of the species *Bos Taurus*. Kevin R. Kaiser concluded that at least some Bes-vases "were possibly used as containers for milk or beef products e.g., milk, butter, cheese, yogurt, broth, fat or meat" [6], blaming protein degradation and extraction protocols for the limited success of the analysis.

After two decades from that unique study, the opportunity to address this issue comes from the identification in the collection of the Tampa Museum of Art (TMA) in Tampa, Florida, of an unpublished example a mug in the form of the head of Bes. In 1984, the TMA acquired a ceramic drinking vessel with a mold-shaped head of Bes, alongside 45 antiquities, from the collection of David S. Hendrick III (1914-2005) (Fig. 1a). The TMA Bes mug, also 3D digitized via structured light 3D scanning by one of the authors (Fig. S1) [14], was purchased at the Maguid Sameda Art Gallery in Cairo on October 20, 1960. It was said to be found in the Fayum district and was tentatively dated by the antiquities dealer to the 2nd century BCE. No further documentation seems to have been provided supporting either the stated provenance or dating. In this 4.5 cm high example from the TMA, accession no. 1984.032, instead of his usual feather crown, the Bes head is topped with a double-rimmed neck with a single vertical loop handle on the right side. The piece belongs to the Type C of the Guidotti classification [15] and GR 1 of the Kaiser seriation [6]. The Tampa object is similar to one example with unknown provenance from the Ghalioungui collection [16] (Fig. 1b) and with another unpublished one from the Allard Pierson Museum (APM inv. no. 14.415) in Amsterdam (Fig. 1c) where there are other four partially preserved pieces (APM inv. nos. 7263 and 14.412–415). Most importantly, the TMA example appears to derive from the same mold used for a Bes mug from the El-Fayūm Oasis [17] (Fig. 1d), a fact that confirms its Egyptian provenience.

To shed light on the role such Bes mugs may have played in the rituals revolving around Bes, contribute to the discussion about their content, and frame their contexts within the mythological traditions, a multidisciplinary analytical study has been conducted on samples extracted from the Ptolemaic-era example at the Tampa Museum of Art.

Results

ATR and SR μ-FTIR results

Figures 2a-c display optical images of the sample collected from vessel residues at varying magnifications. The sample is primarily composed of small grains of different sizes and colors. Among these, certain grains exhibit a brown-black color with an opaque appearance, while others show a translucent aspect with colors ranging from dark orange to pale yellow to white.

In panel d of the figure, the analyzed sample TMA1 corresponds to one of the brown opaque grains. The average spectrum of this sample indicates a strong absorbance peak at approximately 1070 cm^{-1}, likely attributed to the Si-O stretching of silicates. Despite the observed color variations in this sample, all collected spectra exhibit similar features, and no evidence of organic compounds was detected. Therefore, it is reasonable to suggest that the analyzed grain represents a fragment of the ceramic vessel.

Figure 3a displays the optical image of sample TMA2, which exhibits two regions characterized by varying colors. The whitish region, delineated by a red frame, was analyzed, and its average spectrum is primarily composed of gypsum, as indicated by the red line in panel b. Gypsum is a typical environmental contaminant that is commonly found at excavation sites in arid regions. However, it is also possible that it was used in Egyptian ceramic production as plaster or mortar since the predynastic period [18].

The orange-brownish region of the sample comprises a significant proportion of silicates, likely originating from the ceramic matrix of the vessel. However, a group of spectra collected within areas delineated by green frames exhibited complex infrared signals lying underneath the silicate absorption. These signals were likely due to a mixture of one or more organic aromatic substances. An average spectrum (2 - green line in panel b, Fig. 3) was obtained from the aforementioned regions. Since the spectrum was considerably influenced by strong silicate absorptions at approximately 1070 cm^{-1}, the spectrum of the ceramic matrix (average spectrum of sample TMA1, 3 - black line) was subtracted from it to produce the difference spectrum (4 - blue line in panel b). A first attempt of attribution has been done by Wiley SpectraBase software [19], suggesting the presence of harmaline. Additionally, panel b displays the spectrum of the hydroalcoholic extract (5 - purple line) obtained from ground *Syrian rue seeds* (for further details, see the Materials and Methods section). The fingerprint region of these last two spectra has been highlighted in panel b by a dotted frame and zoomed in to enable better recognition of the strong spectral similarities between the ancient compound and the modern extract, as shown in panel d (4 and 5, blue and purple line, respectively).

The main infrared features of the ancient compound and the modern extract exhibited a high degree of similarity with the reference spectrum of harmaline (6 - orange line, panel d and chemical structure in panel c) obtained from reference standard. Additional features were observed, in the archaeological sample and in the modern extract, at approximately 1780 and 1740 cm^{-1}, representing a high-frequency infrared doublet that is characteristic of the stretching vibration of C=O in six-membered cyclic ring acid anhydrides [20]. These additional features may be attributed to fatty or carboxylic acids that are present in *Peganum harmala* [21].

Figure 4a displays average spectra collected from sample TMA3 (2, 4, and 5 - light green, red, and brown lines, respectively) extracted from areas outlined by a green and a red frame in Figure 4b. The sample area within the green frame shows a light orange color and appears to be composed of small fibers. Spectrum 2, collected from this area, exhibits several characteristic absorption bands attributed to wood components (compared to spectrum 1 - deep green line collected from a modern wood reference sample). Specifically, the broad band in the range of 1180-950 cm^{-1}, due to C-O-C, C-O, and C-C stretching

vibrations, is typical of cellulose, while the sharp peak at 1509 cm^{-1} is usually attributed to the aromatic skeletal vibrations of lignin [22]. The increased absorption of the band at around 1640 cm^{-1} in spectrum 2, due to -OH bending moiety, can be attributed to cellulose degradation resulting from hydrolysis [23].

The area outlined by the red frame appears to be deep orange in color. Spectra 4 and 5 (panel a, red and brown lines) exhibit some infrared features like those already observed in spectrum 2, particularly in the spectral region 1180 - 950 cm^{-1}, which is due to carbohydrates. However, these spectra exhibit more intense and defined bands, both in the range 3000 - 2800 cm^{-1} due to CH3-CH2 stretching and in the range 1760 - 1490 cm^{-1}. Specifically, the intense band at 1650 cm^{-1}, accompanied by the bands at 1540 and 1230 cm^{-1}, can be attributed to Amide I, II, and III, respectively, and suggest the presence of proteinaceous compounds [20] or complex molecules composed of both protein and carbohydrate fractions possibly deriving from honey or royal jelly [24] a natural product composed of a complex mixture of proteins, carbohydrates, lipids, and unsaturated fatty acids (see for comparison a royal jelly reference spectrum, panel a, orange line). Additionally, spectrum 5 also displays further features at 1615 and 1320 cm^{-1}, which may be attributed to the presence of some calcium carboxylates such as weddellite. For comparison, reference spectra can be found in the Kimmel Center for Archaeological Science Infrared Standards Library of the Weizmann Institute of Science and the IRUG Spectral Database (ID IMP00425) [25]. To better evaluate the presence of protein fraction, second derivative functions were calculated for spectra 2 and 4 in the range 1900-900 cm^{-1} (figure 4c). The second derivative of spectrum 4 clearly reveals the complex features of the amide I, II, and III bands, which were not detected in spectrum 2. These findings highlight that the two portions of the sample are characterized by the presence of different chemical compounds (or different classes of carbohydrates).

Finally, distinct spectra were obtained from the area of sample TMA3 outlined by the purple frame (panel 4b), which exhibited a whitish appearance. The corresponding average spectrum (3 - violet line, Figure 4d) displayed infrared absorptions around 1600 cm^{-1}, with a peak at 1550 cm^{-1}, accompanied by three sharp and intense peaks at 1440, 1406, and 1390 cm^{-1}, typically associated with antisymmetrical and symmetrical COO- stretching in organic acid salts [26] respectively.

The characteristic doublet at 1100 and 1050 cm^{-1}, typically attributed to C-OH stretching vibrations, suggested a possible identification with sodium or calcium tartrate.

Comparing spectrum 3 with a sodium tartrate reference (spectrum 2 in Figure 4d), shifts and additional features were observed [27], suggesting the possible complexation of tartaric acid with other metallic cations, such as calcium and/or potassium, which are commonly found in ancient wine or fruit juice residues [28]. However, a possible contribution of a citrate salt cannot be ruled out, as demonstrated by the comparison with a sodium citrate spectrum (Figure 4d, spectrum 1) and the detection of citric acid by HPLC-MS analyses (tables 3S and 4S).

Orbitrap Exploris™ HRMS combined Targeted/Untargeted Metabolomics with Compound Discoverer™ Workflow and Proteomic results.

Raw data obtained by LC-Orbitrap-HRMS analysis were processed by Compound Discoverer™ (CD) workflow that was particularly adapted for combined targeted/untargeted profiling of our archaeological sample. Through the integration of both targeted and untargeted metabolomics, a comprehensive list of potential molecules present in the samples was generated and documented in Table S3, along with supplementary Table S4. The combination of these two analytical methods facilitated the acquisition of complementary data, thus optimizing the identification process. Targeted HRMS analysis focuses specifically on known metabolites, while untargeted HRMS profiling encompasses the entire metabolome, enabling the detection of unknown or unexpected metabolites. This combination of approaches offers a more holistic perspective on the unidentified compounds under investigation in samples with complex and extensive histories, such as archaeological artifacts. Employing the platform, a total of 67 compounds were successfully differentiated and classified into the categories detailed in Table S3. Importantly, all identified compounds in Table S4 were verified with a high level of confidence, involving precise mass measurements, the isotopic pattern of the parent ion, and corresponding MS/MS fragmentation.

Alkaloids are the most significant compounds identified in the analysis. Harmaline, harmine, and vasicine were detected through targeted analysis, while their metabolites, such as tetrahydro-harmine and harmol, were identified using a CD data mining element known as the "Compound class scoring node." This element compares the detected m/z values in the fragmentation scans to the fragments found in selected compound class libraries. In the carbohydrate group, special attention should be given to the identification of cellobiose, which serves as the structural unit of cellulose and was revealed through IR technique. Additionally, the presence of chitobiose, with its characteristic fragmentation indicating an N-Acyl-galactosamine unit, suggests its potential as a marker for the polysaccharide chitin. Notably, the structural identification of two gallotannins, namely 1,2,3,6-Tetra-O-galloyl-β-D-glucose and 1-O,6-O-digalloyl-β-D-glucose, is significant since no previous data exists regarding their presence in archaeological pottery.

Valuable information regarding the presence of oxidized fatty acids was obtained through isotopic and fragmentation patterns of parent features (listed in the fatty acid derivative section of Table S3). The heterocyclic, amino acid, and organic acid segments exhibited fragmentation patterns that strongly matched library data. While certain flavonoids such as quercetin and naringenin were specifically targeted, others were discovered through the untargeted approach. Special attention should be given to salipurposide and isosalipurposide, two isomeric compounds with identical fragmentation modes but different retention times (refer to supplementary Table S4).

Lastly, the analysis included three features classified as unknown, despite clear chromatographic characteristics and rich fragmentation patterns. The final structure of these compounds cannot be proposed at this time.

Moreover, in addition to the integration of HRMS analytical strategies for metabolite and small molecules identification, the application of proteomic techniques can provide valuable insights into the biological residues and tissues in the sample under investigation, including a large number of peptides from environmental contamination (the complete list of peptides is available at the repository PXD040739). Proteomics applied to archaeological ceramics residues allows for the identification and quantification of proteins in complex matrices. The integration of proteomic data with metabolomic data led us to identify three different groups of ingredients distinguished by their origin or possible use, such as psychotropic plants, food or related, and human tissues.

aDNA Metabarcoding Sequencing Results

Single-locus plastidial region, *trnL*, have been proposed for the definition of the vegetal component in complex matrix analysis using DNA metabarcoding [29]. In particular, the trnL-g and trnL-h primer set was used to amplify the P6 loop of *trnL* (UAA) for an ethnobotatny genomics approach [30]. Following DNA extraction in a dedicated environment and following SOPs for aDNA analysis, we were able to obtain an amplification signal with only 27 PCR cycles, demonstrating the excellent preservation conditions of the artifact and the efficiency of the sampling method (Fig. 5a). The negative control and mock DNA extractions did not yield any amplification signal until the 50th PCR cycle. Massive amplicon sequencing returned 1,133,062 paired-end raw reads, which we processed bioinformatically to group them by similarity. We identified three main clusters with lengths of 46, 48, and 54 bp, respectively. The gene locus used, apart from its undeniable advantages, has among its shortcomings the taxonomic resolution limited to Family level. The sequence similarity search allowed us to assign these three clusters to the families of *Nitrariaceae*, *Cleomaceae*, and *Nymphaeaceae*, respectively, in order of increasing length (Fig. 5b). A similarity search for all the other less represented clusters always found an association with one of these three families. The most abundant cluster was that of the *Nitrariaceae*, comprising about 64% of the reads, followed by the *Nymphaeaceae* (26%) and *Cleomaceae* (10%). Biological material from these three families has never been analyzed in our laboratory before. While bearing in mind the quantitative limitations of our genetic approach, we believe that the different reads abundances reflect the biomasses used, especially if leaves or otherwise aerial parts of botanicals was used in the infusion composition.

Discussion

The analyses conducted have revealed a rather complex composition for the concoction contained in the Bes-vase from the Tampa Museum of Art.

With respect to findings related with plant-based substances, the *Peganum harmala L.*, belonging to the Nitrariaceae family, and commonly known as *harmel* or *Syrian rue*, stands out. It is a medicinal and psychoactive plant that is native to the Mediterranean basin, Near East, since pre-Islamic times [31], and part of Asia [32]. The seeds of this plant produce high quantities of the alkaloids harmine and harmaline, which induce dream-like visions, considered of the oneirophrenic kind [33], and in lower concentrations of the alkaloid vasicine, which has utero-tonic properties able, at certain dosage, to aid childbirth or induce

abortion as confirmed by modern pharmacological research [34]. Although the identification of *harmel* in Egyptian hieroglyphic texts is uncertain and its identification with the plant *ḏaajs* has been only dubitatively suggested [35, 36], the oldest evidence of human use of *P. harmala* in Egypt can be traced back to the pre-Dynastic period through the discovery of seeds dated to 3700-3500 BCE [37]. In the 2nd to 4th century CE, it still seems to be used in Coptic rituals related to the Tree of Life [38]. Various ancient and modern names for *harmel* have roots that are constituted by the set of letters *bs-* and *bss-*, including *baššāšā* (ancient Syria), *baššūšā* (modern Syria), *bešaš* (ancient Aramaic), *basous* (Coptic), *bêsasa* (modern Egypt), and *bêsa* (Greek Medical Papyri) [36]. The names *bêsa* and *bêsasa* have been traced to that of Bes, and have been interpreted as the "plant of Bes" [39,40]. A ritual linked to the cult of Bes during the Greco-Roman periods involved the practice of incubation for oracular purposes, in which the consultants slept in the Bes-Chambers at Saqqara to obtain prophetic dreams. This practice was mentioned in the late imperial writings of Ammianus Marcellinus (*Res Gestae* 19,12.3-12) in relation to the Oracle of Bes at Abydos, and an archaeological testimony is based on hundreds of Greek language graffiti that were engraved by the oracle consultants on the walls of the temple of Seti I in Abydos. In these graffiti, Bes is referred to as the "*giver of oracles*" and "*giver of dreams.*" The oracle of Abydos was active from the 1st or 2nd to the 5th century CE, and other evidence of oracle dreams of Bes can be found in the *Greek Magical Papyri* from the same late imperial period [41,42]. The oneirophrenic effects of *harmel* would be well-suited for these incubation practices.

In addition to the etymological and biochemical data that associate Bes with *P. harmala*, iconographic evidence shows that this deity was also associated with another psychoactive plant, the blue water lily (*Nymphaea nouchali* Burm. f. var. *caerulea* (Sav.) Verdc., Nymphaeaceae family, improperly known as "blue lotus"). Our biochemical analysis has reinforced this association. At least twelve figurines of Bes emerging from a blue water lily flower are known [43], and representations of this flower can be found on different types of Bes-vessels (e.g., [4], figs. 1-11). Water lilies have long been used as a food source and are still consumed in various regions of Africa and Asia. Even in Egypt, the fruits, seeds, and rhizomes of water lilies are used to produce flour for food, although the earliest references to this practice do not predate the Greco-Roman period [44]. Several species of water lilies are considered to have "narcotic and sedative" properties and have been traditionally used as medicines and for their intoxicating effects, as it emerges for the African ethnographic literature [45,46,47]. Regarding the active compounds of water lilies, some chemical studies have reported the presence of alkaloids with an aporphine structure in the flowers and rhizomes [48].

The HRMS analysis conducted, primarily focusing on the identification of markers related to other types of plants offered data for the use of a possible recipe. The data presented in Table S3 indicate a significant presence of beta-carbolines, quinazoline alkaloids, and other alkaloids typically found in psychoactive plants. Specifically, the presence of harmaline, harmine, vasicine, and ruine together are characteristic of *Peganum harmala* seeds [21,49,50], along with other degradation products of these molecules. Additionally, psychoactive alkaloids such as nupharidine and probably also neferine (with low

signal) are found in plants belonging to the Nymphaeaceae family [51–53]. The presence of a series of flavonoids, including dyes, further supports the molecular fingerprint of *Nymphaea nouchali* Burn. f. var. *caerulea* (Sav.) Verdc.

Tannins may not be fully explained by the archaeological context, but their presence confirms the use of plant-based materials. Lignin, detected with SR µ-FTIR, shows a potential correlation with other degradation products by enzymatic action [54], identified through HRMS. These compounds, including p-coumaric, 4-hydroxyphenylacetic, gentisic, ferulic, and isoferulic acids, are also synthesized via the phenylpropanoid biosynthetic pathway in plants [55].

Establishing a direct link between the detected flavonoids and the plants identified through cDNA analysis is challenging since many of these compounds are common among different flowers and seeds. Nonetheless, the flavonoid data are consistent with the presence of honey residues [56]. The detection of chitobiose, indicating the presence of insect exoskeletons, could be attributed to *Drosophila melanogaster*, as proposed by proteomics analysis. Additionally, it is conceivable that salipurposide and isosalipurposide originate from grape skins [57], which, when accompanied by galotannins and the identification of tartaric salts through SR µ-FTIR, suggests the presence of fermented products.

The identification of 18-β-Glycyrrhetinic acid, a naturally occurring triterpenoid abundantly found in the roots of licorice (*Glycyrrhiza glabra*) [58] and other plants belonging to the Glycyrrhiza genus, suggests the potential presence of this plant. Although, it is challenging to find direct evidence in the literature regarding the cultivation of licorice in ancient Egypt, its presence cannot be entirely dismissed [59].

The presence of long-chain polyhydroxylated acids, such as 9,12,13-TODEA, 12,13-DIHOME, and 9-HODE, indicates that, despite the highly heterogeneous nature of the organic residues, components of vegetable origin might also be present. Previous studies have documented that the presence of oxidation products derived from distinct unsaturated fatty acids suggests the existence of some form of edible oil [60]. Moreover, the readily detectable m/z value and specific fragmentation pattern have revealed the occurrence of pinolenic acid. The presence of pinolenic acid indicates sources rich in this fatty acid, such as pine nuts or pine nut oil [60]. Although ancient Egyptians had access to a variety of plant-based resources, including pine trees, the specific utilization of pinolenic acid-rich sources in their ritual practices is not extensively documented in the available literature.

With regards to the third sequence tag identified, we have obtained a list of ten plants that match 100% with the chloroplast aDNA. All the species on this list belong to the Cleomaceae family, some of which were formerly classified under the Capparidaceae family. In Egypt, ten native species of *Cleome* are recognized [61], two of which are present in this list: *C. gynandra* and *C. chrysantha*. Archaeological findings of *Cleome* species have been discovered throughout Egypt, from Predynastic to Coptic times. For example, charred remains of a plant identified as *Cleome/Gynandropsis* type have been found in a Neolithic (6000 BCE) house at the Nabta Playa site, Southern Egypt [62]. Remains of *C. droserifolia* (Forssk.) Delile and *C. paradoxa* R.Br. ex DC. have also been found in various Roman to Coptic sites [63].

Among the plants on the list, *Cleome gynandra* L., also known as *Gynandropsis gynandra* (L.) Briq., is the most interesting. It is widely used in Africa for various medicinal purposes. Its fresh roots, when taken orally, serve as a promoter of labor, while its leaves, also when taken orally, serve as an abortifacient and oxytocic [64]. Infusions of the leaves are also used to facilitate birth [65]. These properties are like those of *Peganum harmala*, and the difference between the promoter of labor and the abortifacient properties for both plants depend on the quantities used.

Cleome chrysantha Decne., another plant on the list, was found in nine desiccated seeds in a Predynastic trash mound at Hierakonpolis, Southern Egypt, around 3800-3500 BCE [66,67]. In Egypt, this species is used in traditional medicine as an anthelmintic (used to treat parasitic worms) and to treat infantile convulsions [68].

Through microscopy, we identified crystallizations of harmaline and the possible presence of the tartaric acid salts in the same sample using SR-µFT-IR. These findings confirm the presence of a fermented alcoholic liquid derived from fruit. However, the absence of other specific markers, such as proline, malvidin, and syringic acid for grape wine [69,70], or pomegranate markers, as reported in a previous study [71], and the complexity of the sample did not allow us to determine the exact origin of the fermented product, with a high compatibility for a grape-derived liquid due to the presence of salipurposide and isosalipurposide.

Through genetic investigations conducted specifically on chloroplast aDNA, we were able to confirm the presence of at least three plants belonging to the families Peganum and Nitraria, Nuphar and Nymphaea, and Tarenaya, Sieruela, and Gynandropsis. Combining all these data, we can conclude that *Peganum harmala* and *Nymphaea caerulea* plants were deliberately used as sources of psychoactive substances for ritual purposes.

In addition to plant-based substances, proteomic analyses indicated a high presence of human proteins within the residue. This is normally classified as contamination, and again most of the human skin proteins detected were classified as contaminants (refer the raw data for the complete list of proteins detected). Nonetheless, we identified several other proteins, such as Mucin-5B (Q9HC84, in particular peptides GYQVCPVLADIECR, AQAQPGVPLR, EEGLILFDQIPVSSGFSK, ELGQVVECSLDFGLVCR, VCGLCGNFDDNAINDFATR), Lactotransferrin (P02788, in particular peptides LADFALLCLDGK SVQWCAVSQPEATK, YLGPQYVAGITNLK, DVTVLQNTDGNNNEAWAK, EDAIWNLLR, ESTVFEDLSDEAER, FDEYFSQSCAPGSDPR, FQLFGSPSGQK, GGSFQLNELQGLK, LRPVAAEVYGTER, SDTSLTWNSVK, VVWCAVGEQELR), Prolactin-inducible protein (P12273, in particular the peptides FYTIEILKVE, ELGICPDDAAVIPIK, ELGICPDDAAVIPIKNNR, TYLISSIPLQGAFNYK), Serum albumin (P02768, in particular AVMDDFAAFVEK, ADDKETCFAEEGK, ADDKETCFAEEGKK, QEPERNECFLQHKDDNPNLPR, TYETTLEK), Hemoglobin subunit beta (P68871, peptide FFESFGDLSTPDAVMGNPK), and Gamma-glutamylcyclotransferase (O75223, peptide DVTGPDEESFLYFAYGSNLLTER), suggesting a deliberate addition of human fluids to the drink prepared for ritual purposes. This includes fluids like breast milk, mucous fluids (oral or vaginal), and blood.

On the other hand, the analysis of non-human proteins also showed the use of various other ingredients, such as honey or royal jelly, as also suggested by SR μ-FTIR analyses. The presence of Arginine kinase (O61367, peptide EMHDGIAELIK) indicated the use of honey and honey-related products (like royal jelly), as this protein is a widely used marker for recognizing its origin [72,73]. Additionally, traces of common wheat (*Triticum aestivum*) and sesame seeds (*Sesamum indicum*) were found, along with yeasts from fermentation, such as *Saccharomyces cerevisiae* (strain ATCC 204508/S288c) and *Schizosaccharomyces pombe* (strain 972/ATCC 24843). Numerous *Drosophila melanogaster* proteins were also detected, indicating a high sugar content from honey or fruit. All these proteins exhibit a calculated deamidation level of at least 20%, which distinguishes them from other contamination proteins that display a deamidation level of less than 6% and are thus not included here. The evaluation of the deamidation index provides a useful means of distinguishing ancient proteins from modern ones [74]. Proteins from *P. harmala*, *N. nouchali*, and Cleome species were not detected. This could be due to several factors: plant preparation methods leading to lower protein concentration and higher alkaloid concentration, protein degradation over time, and limited availability of species-specific peptides and proteins in reference databases. To address this issue, a multi-technique approach, as demonstrated in this study, is recommended to minimize biases and achieve a comprehensive characterization from multiple perspectives [27,75–77]. Moreover, the proteins listed in Table S1 have been assigned to their respective species based on all identified peptides, where at least one sequence exclusively belongs to one specie, using a functional metaproteome analysis by the UniPept 5.0.8 database to determine the lowest common ancestor [78].

The multimodal analytical approach applied for the characterization of the organic composition of the residual liquid concoction contained in the Bes-vase from the Tampa Museum of Art revealed a mixture of nutraceutical, medicinal, psychotropic, and biological substances used in an otherwise unattested ritual (Table 1). In conclusion, recalling the tale told in the Myth of the Solar Eye and in the light of our results, it would be possible to infer that this Bes-vase was used for some sort of ritual of reenactment of what happened in a significant event in Egyptian myth. Expanding the sampling chemical study to other examples of similar and contemporaneous Bes-vases becomes at this point critical to ascertain if the evidence here discussed was a rare or single event, or a widespread practice at least for the Ptolemaic period.

Materials and Methods

Pottery samples were ground and weighed. Gloves and a mask were worn during all steps of the protocols.

ATR and SR μ-FTIR Methods

Microscopic observation and Fourier Transformed Infrared (FTIR) analyses were conducted at the Chemical and Life Sciences branch (SISSI-Bio) of the SISSI beamline at Elettra Sincrotrone Trieste in Italy [79].

Optical images were collected with a ZEISS Stemi 305 stereo microscope available at the beamline, showing that the sample collected from the Bes vessel had a very heterogeneous appearance, consisting of small orange-brownish fragments, some of which characterized by a translucent crystalline appearance.

Synchrotron radiation-based µ-FTIR measurements were performed using a Vis-IR Bruker Hyperion 3000 microscope coupled with the Vertex 70v interferometer in the MidIR range (MCT-A detector, 4,000−650 cm^{-1}). The sample was analyzed in triplicate by collecting few grains and pressing them in a diamond compression cell (Diamond EX press by S.T. Japan, clear aperture 2 mm) to obtain a suitable thickness for µ-FT-IR measurements in transmission mode. The triplicates were identified as TMA1, TMA2, and TMA3.

Thirty to forty spectra were collected for each triplicate, averaging 512 scans for each spectrum, at 4 cm^{-1} spectral resolution and setting the lateral resolution at 15×15 µm to select the most diagnostic sample regions according to the observable differences in color.

FTIR measurements in Total Attenated Reflection (ATR) mode were performed on standard samples, used as references. Among the standards, dried *Peganum harmala* seeds were purchased in 2021 from the company *VisioneCurativa − Ethnobiology and Research* (Italian VAT 01943220895, Monte Bongiovanni snc, Sortino, Italy), and 3 mg were ground in an agate mortar and dissolved in a 1 mL 70% (v/v) alcoholic solution. A volume of 5 µL of the supernatant was analyzed in triplicate after 30 minutes and after 24 hours. Harmaline and sodium L-tartrate dibasic dihydrate powders were supplied by Sigma-Aldrich, and sodium citrate tribasic dihydrate was from Fluka. The standard powders were analyzed in triplicate. The modern wood standard sample was purchased from El-Orman Botanical Garden (Giza, Egypt).

Both solutions and powders were analyzed using a Bruker Vertex 70 interferometer, collecting 256 scans at a spectral resolution of 4 cm^{-1} in the MidIR range (DTGS detector, 4,000−500 cm^{-1}).

All the collected spectra were preprocessed using Bruker OPUS 8.5 software. The spectra of the standards were averaged, and a 16 pt. rubberband baseline was applied. Average spectra were extracted from the most representative areas of the sample TMA1, TMA2, and TMA3, selected based on their differences in color. All the extracted spectra were preprocessed as described above for the standard ones. Second derivative spectra were calculated by applying 17 pt. smoothing. The most representative spectra were plotted using Origin Pro 2020 9.7 software (Origin Lab, Ltd., Northampton, MA, USA).

Proteomics Methods

To account for the extensive protein degradation, 50 mg of ground pottery underwent a basic peptide extraction following the protocol reported in [76,77]. Initially, 200 µl of 50 mM triethylammonium bicarbonate (TEAB) was added to the ground pottery and vortexed thoroughly for ten minutes at room temperature. The mixture was then sonicated for five minutes and centrifuged, after which the supernatant was transferred to a clean centrifuge tube. Next, to solubilize hydrophobic peptides, 200 µl of

50/50 acetonitrile/water was added, vortexed for ten minutes, sonicated, and centrifuged. The resulting supernatants were combined and dried using a speed vacuum. Finally, peptide extractions were re-suspended in H_2O + 5% trifluoroacetic acid (TFA), desalted using C18 columns in a vacuum manifold, and again dried using a speed vacuum.

Another 50 mg of ground pottery were solubilized for trypsin digestion using 200 μl of 5% w/v sodium dodecyl sulfate (SDS) in 50 mM TEAB. Protein concentrations were determined using the 660 Protein Assay (Pierce). Equal amounts of protein were processed for LC-MS/MS using s-traps (Protifi) following the protocol reported in [80] and [81]. Briefly, proteins were reduced with dithiothreitol (DTT), alkylated with iodoacetamide (IAA), acidified using phosphoric acid, and combined with s-trap loading buffer (90% methanol MeOH, 100 mM TEAB). Proteins were loaded onto s-traps, washed, and finally digested with Trypsin/Lys-C (1:100, w:w; enzyme:protein) overnight at 37°C. Peptides were eluted and dried using a speed vacuum.

Peptides were resuspended in H_2O: 1% acetonitrile: 0.1% formic acid for LC-MS/MS analysis. Chromatographic separation of peptides was performed using an Ultimate3000 UHPLC (Thermo Scientific, San Jose, CA, USA) with a Thermo Acclaim PepMap 75 μm x 50 cm C18 reversed-phase-HPLC analytical column (Thermo Scientific). The column oven temperature was set to 50°C, and with a flow rate of 300 μL/min. Mobile phases used for peptide separation are A: H_2O: 0.1% formic acid, and B: acetonitrile: 0.1% formic acid; gradient elution began at 2% B, increasing to 32% B over 60 minutes.

High-resolution mass spectrometry was performed using a hybrid quadrupole-Orbitrap mass spectrometer (Q-Exactive Plus, Thermo Fisher Scientific), equipped with a Nanospray Flex Ion Souce (Thermo Scientific, San Jose, CA, USA).   Instrument calibration was performed using Pierce LTQ Velos ESI Positive Ion Calibration solution (Thermo Scientific, San Jose, CA, USA) prior to the analysis of the TMA sample. The capillary temperature was set at 325°C. The spray voltage was set to 2.4 kV for positive mode; sheath and auxiliary gas were both set at 0 arbitrary units. The S-lens RF level was set at 55.

The analysis was performed in positive mode, using data-dependent acquisition (DDA). Full MS survey scans were acquired at a resolution of 70,000, scan range 375-1500 m/z, automatic gain control (AGC) target 1e6 ions, and a maximum injection time (IT) of 50ms. The top 10 most abundant ions were selected for MS/MS fragmentation and detection. MS/MS scans were acquired at a resolution of 17,500, AGC target 5e4 ions, maximum IT of 50ms, with an isolation window of 1.5 m/z, and a normalized collision energy (NCE) of 28. A dynamic exclusion window of 45 seconds was included in the method.

The raw data files were processed in MaxQuant (v 1.6.14.0, www.maxquant.org) and searched against the vertebrate protein sequences database first and then the entire UniProtKB reference proteome database.   Search parameters included constant modification of cysteine by carbamidomethylation and variable modifications methionine oxidation, protein N-term acetylation, and asparagine or glutamine

deamidation.   Proteins were identified using the filtering criteria of 1% protein and peptide false discovery rate. The protein intensity values were normalized using the MaxQuant LFQ function [82].

Orbitrap Exploris™ HRMS combined Targeted/Untargeted Metabolomics with Compound Discoverer™ Workflow.

30 mg of powder was dissolved in a mixture of methanol and water (70:30) at a volume of 1 mL and vortexed for 3 minutes. The resulting solution was sonicated for 10 minutes and then centrifuged at 5500 RCF at 5°C for 10 minutes. The supernatant was then transferred to a vial, and 2 µl was injected for HPLC-HRMS analysis using the Vanquish/Orbitrap Exploris 120 platform.

Chromatographic separation was performed using a Vanquish HPLC instrument (Thermo Fisher Scientific, Germering, Germany) with a Thermo Accucore aQ 100x2.1 mm, 2.6 µm column and a programmed gradient flow (300 µL/min) of 0.1% formic acid (HCOOH) in water (A) and acetonitrile (B). Gradient elution began at 5% B, was increased to 15% B in 1.2 min, and to 98% B in 12.5 min, with a holding time of 5 min. Initial conditions were reached in 0.5 min, and the system was stabilized for 5 min. The total run time was 23 min.

An Orbitrap Exploris™ 120 (Thermo Scientific, San Jose, CA, USA) equipped with a heated electrospray ionization source (HESI, Washington, DC, USA) was used for high-resolution mass spectrometry detection. The analysis was performed separately in positive and negative acquisition modes, with optimized acquisition parameters. Instrument calibration was carried out with a direct infusion of a Pierce FlexMix Calibration solution (Thermo Scientific, San Jose, CA, USA). Capillary temperature and vaporizer temperature were set at 300°C and 320°C, respectively. The HESI spray voltage was set to 3.3 kV for positive mode and 3.2 kV for negative mode; sheath and auxiliary gas were set at 40 and 10 arbitrary units, respectively. The full scan acquisition mode was selected with a resolution of 120,000 FWHM, a scan range of m/z 150-850, and an automatic gain control (AGC) set in the standard mode, with an automatic maximum injection time and an RF lens level of 70%, and micro-scans of 1.

Full scan data-dependent MS2 acquisition (FS-dd-MS2) with a resolving power of 120,000 and 30,000 for FS and dd-MS2, respectively, was employed for fragmentation of pseudo-molecular ions or adducts detected in FS mode. The full scan acquisition mode was selected with scan range of m/z 150-850 Th. The FS-ddMS2 was set for targeted molecules (total of 10 compounds) with the option to perform fragmentation on the most intense untargeted ions if targeted ions were not present. Therefore, the HRMS detection workflow was based on a combination of targeted/untargeted principles. Fragmentation of precursors was executed with stepped, normalized collision energy (NCE) set at 20, 40, and 80%.

The Exploris Orbitrap raw data were submitted to Compound Discoverer (CD) 3.3 software (Thermo Fisher, San Jose, CA, USA), which enabled the programmed identification and relative abundance of compounds. The procedure was based on two CD workflows: 1) Untargeted/targeted metabolite identification, which comprised a sequence of steps that were accomplished consecutively, including spectra selection, retention time alignment, peak detection, profile assignment, and isotope annotation,

and 2) Expected compounds evaluation, which included the list of predictable molecules and their eventual transformation. The putative identification was accomplished by consulting CD-integrated databases (https://www.mzcloud.org and https://www.chemspider.com), accompanied by two different types of mass lists: those performed in-house and those available in online database relative to food and toxicology sectors. The criteria for putative identification of metabolites identified by the CD workflow were chosen as a combination of a few different assets: mzCloud (Thermo Fisher, Bratislava, Slovakia) match score higher than 80% (cosine match algorithm) and the same identification being proposed by at least one external web database, such as the Human Metabolome platform HMDB (https://hmdb.ca/), the Kyoto Encyclopedia of Genes and Genomes (KEGG) (https://www.genome.jp/kegg), Pubchem (www.pubchem.com), the Small Molecule Pathway Database (SMPDB) (http://smpdb.ca), and lipid maps (https://www.lipidmaps.org). If the mass fragmentation pattern did not match any of the available library, the fragmentation pattern was evaluated by FISh (Fragment Ions Shearch) Scoring (implemented in Compound Discoverer) compared with recent publications.

aDNA Sequencing Methods

16 mg of powder material recovered from the vase was processed for nucleic acid extraction in a laboratory area dedicated to the analysis of ancient DNA (aDNA). A brand-new commercial kit, Quick-DNA Plant/Seed Kits (ZymoResearch), was used to extract the DNA, which was eluted in a volume of 50 μL. To ensure there were no possible contaminations, mock extractions without samples were systematically performed. DNA amplifications were conducted in a final volume of 25 μL, using 5 μL of undiluted DNA extract as the template. The amplification mixture contained 12.5 μL of AccuStart™ II PCR ToughMix (Quantabio), 0.1 μM of each primer, and 1 Evagreen to monitor the amplification kinetics on a BIO-RAD CFX96 thermal cycler. The mixture was denatured at 94°C for 3 minutes, followed by cycles of 15 seconds at 94°C, 10 seconds at 55°C, and 20 seconds at 72°C. The P6 loop region of the trnL (UAA) intron was amplified in triplicate using the universal primers g (5'-GGGCAATCCTGAGCCAA-3') and h (5'-CCATTGAGTCTCTGCACCTATC-3'), which were modified by the addition of an adapter sequence (Illumina, San Diego, CA, USA) on the 5' ends [83]. Amplicon sequencing was performed using the 2 × 150-bp paired-end method on the MiSeq platform with a MiSeq Reagent Kit v2 Nano (Illumina). The reads obtained from the sequencing were processed using the CLC Genomics Workbench software environment ver. 22.0. Specifically, the reads were subjected to quality control and adapter/primer trimming, followed by clustering with a De Novo approach using the OTU clustering tool of the CLC Microbial genomics package. Finally, sequence similarity searches of the representative sequences were performed via BLASTn analysis on the nucleotide GenBank non-redundant database. All raw read data of this study are available under DOI 10.5281/zenodo.7954932 [84].

Declarations

Data availability

3D model produced in structured light 3D scanning via an Artec Eva. Tampa Museum of Art, accession number 1984.032 Drinking vessel in shape of Bes head; Fayum Oasis, Egypt; Graeco-Roman period (c.3rd cent. BCE-3rd cent. CE). Donated by of David S. Hendrick III (1914-2005): https://skfb.ly/oFApP

Proteomics: ProteomXchange Database PXD040739

Genetic sequences: 10.5281/zenodo.7954932

HMRS spectra reported in Supplementary material.

Competing Interest Statement: The authors declare no competing interests.

References

1. Hedges, A. The Egyptian Dionysus: Osiris and the development of theater in Ancient Egypt. in *XI International Congress of Egyptologists: Florence Egyptian Museum* 271–275 (2017). doi:10.2307/j.ctv177tjnf.52.
2. Gordon, R. *Religion: Greek Religion. Greece and Rome* vol. 48 (2001).
3. van Oppen de Ruiter, B. F. Lovely Ugly Bes! Animalistic Aspects in Ancient Egyptian Popular Religion. *Arts* 9, 51 (2020).
4. Gill, J. C. R. A Corpus of Late Period and Ptolemaic Bes-Vessels from Mut El-Kharab, Western Desert of Egypt. in *Vienna 2 – Ancient Egyptian ceramics in the 21st century. Proceedings of the international conference held at the University of Vienna, 14th-18th of May, 2012.* 211–228 (2012).
5. Dasen, V. Dwarfs in ancient Egypt and Greece. (2013).
6. Kaiser, K. R. Water, Milk, Beer and Wine for the Living and the Dead: Egyptian and Syrio-Palestinian Bes-Vessels from the New Kingdom through the Graeco-Roman period. (University of California, Berkeley, 2003).
7. Defernez, C. Four Bes vases from Tell el-Herr (North-Sinai): analytical description and correlation with the Goldsmith's art of Achaemenid tradition. (2011).
8. Marchand, S. A funny Bes vase!: Early fourth century BCE, Ayn Manāwir, Kharga Oasis. in *Dust, demons and pots* (eds. Warfe, A. R., Gill, J. C. R., Hamilton, C. R., Pettman, A. J. & Stewart, D. A.) 493–502 (Peeters, 2020).
9. Gyôry, H. Remarques sur les vases décorés avec la figure du Bès. in *Egyptian Pottery: Proceedings of the 1990 Pottery Symposium at the University of California, Berkeley* (eds. Keller, C. & Redmount., C.) 114–123 (2003).
10. Schneider, H. D. *et al.* The Tomb of Maya and Meryt: Preliminary Report on the Saqqara Excavations, 1990–1. *J. Egypt. Archaeol.* 77, 7–21 (1991).
11. Woolley, C. L. A North Syrian cemetery of the Persian period. *Ann. Archaeol. Anthropol.* VII, 115–129 (1916).

12. Quibell, J. E. Excavations at Saqqara (1905-1906). *Serv. des Antiq. l'Égypte* (1907).

13. Bleiberg, E. & Pinch, G. Votive Offerings to Hathor. *J. Am. Orient. Soc.***118**, 569 (1998).

14. (IDEx), U. I. for D. E. Drinking vessel in shape of Bes head. https://skfb.ly/oFApP (2021).

15. Guidotti, M. C. Ipotesi di significato e tipologia dei vasi egizi di epoca tarda raffiguranti il dio Bes. *Egitto e Vicin. Oriente***6**, 33–65 (1983).

16. Ghalioungui, P. & Wagner, G. Terres cuites de l'Egypte gréco-romaine de la collection P. Ghalioungui. *Mitt. Dtsch. Archaeol. Inst. Abt. Kairo***30**, 189–198 (1974).

17. Kaufmann, C. *Ägyptische terrakotten der griechisch-römischen und koptischen epoche vorzugsweise aus der oase El Faijūm (Frankfurter sammlung)*. (1913).

18. Harrell, J. A. Amarna gypsite: A new source of gypsum for ancient Egypt. *J. Archaeol. Sci. Reports***11**, 536–545 (2017).

19. Harmaline - Optional[ATR-IR] - Spectrum - SpectraBase. https://spectrabase.com/spectrum/8BpQZX3hitH.

20. Socrates, G. (George). *Infrared and Raman characteristic group frequencies: tables and charts*. (Wiley, 2001).

21. Kartal, M., Altun, M. L. & Kurucu, S. HPLC method for the analysis of harmol, harmalol, harmine and harmaline in the seeds of Peganum harmala L. *J. Pharm. Biomed. Anal.***31**, 263–269 (2003).

22. *Wood production, wood technology, and biotechnological impacts*. (Göttingen University Press, 2007). doi:10.17875/gup2007-262.

23. Łojewska, J., Miśkowiec, P, Łojewski, T. & Proniewicz, L. M. Cellulose oxidative and hydrolytic degradation: In situ FTIR approach. *Polym. Degrad. Stab.***88**, 512–520 (2005).

24. Lazarevska, S. & Makreski, P. Insights into the infrared and Raman spectra of fresh and lyophilized royal jelly and protein degradation IR spectroscopy study during heating. *Maced. J. Chem. Chem. Eng.***34**, 87 (2015).

25. *Infrared and Raman Users Group Spectral Database. 2007 ed. Vol. 1 & 2.: IRUG*. (Infrared and Raman Users Group Spectral Database.).

26. Filopoulou, A., Vlachou, S. & Boyatzis, S. C. Fatty Acids and Their Metal Salts: A Review of Their Infrared Spectra in Light of Their Presence in Cultural Heritage. *Molecules***26**, 6005 (2021).

27. Tanasi, D. *et al.* 1H-1H NMR 2D-TOCSY, ATR FT-IR and SEM-EDX for the identification of organic residues on Sicilian prehistoric pottery. *Microchem. J.***135**, 140–147 (2017).

28. Drieu, L. *et al.* Is it possible to identify ancient wine production using biomolecular approaches? *STAR Sci. Technol. Archaeol. Res.***6**, 16–29 (2020).

29. Taberlet, P. *et al.* Power and limitations of the chloroplast trnL (UAA) intron for plant DNA barcoding. *Nucleic Acids Res.***35**, e14–e14 (2007).

30. Newmaster, S. G. & Ragupathy, S. Ethnobotany genomics - discovery and innovation in a new era of exploratory research. *J. Ethnobiol. Ethnomed.***6**, 1–11 (2010).

31. Schwartz, M. On Haoma, and its Liturgy in the Gathas. in *Proceedings of the 5th Conference of the Societas Iranologica Europaea* vol. 1 215–224 (2006).

32. Lansky, E. S., Lansky, S., Paavilainen, H. M. & Weil, A. *Harmal: The genus Peganum. Harmal: The Genus Peganum* (2017). doi:10.1201/9781315118758.

33. Naranjo, C. Psychotropic properties of the harmala alkaloids. *United States, Public Heal. Serv. Publ.***No. 1645**, 385–391 (1967).

34. Shapira, Z., Terkel, J., Egozi, Y., Nyska, A. & Friedman, J. Abortifacient potential for the epigeal parts of Peganum harmala. *J. Ethnopharmacol.***27**, 319–325 (1989).

35. Miller, R. L. Daajs, Peganum harmala L. *Bull. l'Institut Français d'Archéologie Orient.***94**, 349–357 (1994).

36. Samorini, G. Psychoactive Plants in the Ancient World. in *The Routledge Companion to Ecstatic Experience in the Ancient World* 73–89 (Routledge, 2021). doi:10.4324/9781003041610-7.

37. van Zeist, W. & de Roller, G. J. Plant remains from Maadi, a predynastic site in lower Egypt. *Veg. Hist. Archaeobot.***2**, 1–14 (1993).

38. DuQuesne, T. *A Coptic Initiatory Invocation:(PGM IV 1-25); an Essay in Interpretation with Critical Text, Translation, and Commentary.* (Darengo, 1991).

39. Hopfner, T. *Griechisch-ägyptischer Offenbarungszauber/2, 2.* (Hakkert, 1990).

40. Rahner, H. *Greek myths and Christian mystery.* (1971).

41. Dunand, F. La consultation oraculaire en Égypte tardive. L'oracle de Bès à Abydos. in *Oracles et prophéties dans l'antiquité* (ed. Heintz, J.-G.) 65–84 (De Boccard, 1997).

42. Bortolani, L. M. The Oracle of Bes at Abydos and the 'Dream-Oracle of Bes' in the Magical Papyri: From Sacred Site to a Magical Ritual?. *Simblos 6* 263–281 (2015).

43. Doetsch-Amberger, E. Bes auf der Blüte. in *U Verhoeven & E Graefe (Hersg.) Religion und Philosophie im Alten Ägypten.* 123–128 (Orientalia Lovaniensa Analecta Leuven, 1991).

44. Pommerening, T., Marinova, E. & Hendrickx, S. The Early Dynastic origin of the water-lily motif. *Chron. d'Egypte***85**, 14–40 (2010).

45. Sobiecki, J. F. A review of plants used in divination in southern Africa and their psychoactive effects. *Southern African Humanities* vol. 20 333–351 (2008).

46. Schmid, R. & Neuwinger, H. D. African Traditional Medicine: A Dictionary of Plant Use and Applications, with Supplement: Search System for Diseases. *Taxon***50**, 310 (2001).

47. Das, D. R., Sachan, A. K., Mohd, S. & Gangwar, S. S. Nymphaea Stellata: a Potential Herb and Its Medicinal Importance. *J. Drug Deliv. Ther.***2**, (2012).

48. Oliver-Bever, B. Medicinal plants in tropical west africa II. Plants acting on the nervous system. *J. Ethnopharmacol.***7**, 1–93 (1983).

49. Wang, Z. *et al.* Analysis of alkaloids from Peganum harmala L. sequential extracts by liquid chromatography coupled to ion mobility spectrometry. *J. Chromatogr. B Anal. Technol. Biomed. Life Sci.***1096**, 73–79 (2018).

50. Chabir, N. *et al.* Seeds of Peganum Harmala L. Chemical Analysis, Antimalarial and Antioxidant Activities, and Cytotoxicity Against Human Breast Cancer Cells. *Med. Chem. (Los. Angeles).***11**, 94–101 (2014).

51. Liu, R. M., Xu, P., Chen, Q., Feng, S. ling & Xie, Y. A multiple-targets alkaloid nuciferine overcomes paclitaxel-induced drug resistance in vitro and in vivo. *Phytomedicine***79**, 153342 (2020).

52. Yoshpa, M. Ethnobotany and Phytochemistry of the sacred blue lily of the Nile, Nymphaea caerulea Savigny, Nymphaeaceae (PhD Thesis). (2004).

53. Selvakumari, E., Shantha, A., Kumar, C. S. & Purushoth Prabhu, T. Phytochemistry and Pharmacology of the Genus Nymphaea. *J. Acad. Ind. Res.***5**, 98 (2016).

54. Zhao, L. *et al.* Biological degradation of lignin: A critical review on progress and perspectives. *Ind. Crops Prod.***188**, 115715 (2022).

55. Dixon, R. A. *et al.* The phenylpropanoid pathway and plant defence-a genomics perspective. *Mol. Plant Pathol.***3**, 371–390 (2002).

56. Leoni, V. *et al.* Multidisciplinary analysis of Italian Alpine wildflower honey reveals criticalities, diversity and value. *Sci. Rep.***11**, 19316 (2021).

57. Fernández-Fernández, A. M. *et al.* Tannat Grape Skin: A Feasible Ingredient for the Formulation of Snacks with Potential for Reducing the Risk of Diabetes. *Nutrients***14**, 419 (2022).

58. Ralla, T. *et al.* Investigations into the Structure-Function Relationship of the Naturally-Derived Surfactant Glycyrrhizin: Emulsion Stability. *Food Biophys.***15**, 288–296 (2020).

59. Loftin, H. King Tut's Black Treasure. *Sci. News-Letter***64**, 90 (1953).

60. Colombini, M. P., Giachi, G., Modugno, F. & Ribechini, E. Characterisation of organic residues in pottery vessels of the Roman age from Antinoe (Egypt). *Microchem. J.***79**, 83–90 (2005).

61. Kamel, W., El-Ghani, M. A., Biotechnol, M. E.-B.-A. J. P. S. & 2010, U. Cleomaceae as a Distinct Family in the Flora of Egypt. *Afr J Plant Sci Biotechnol***4**, 11–16 (2010).

62. Mitka, J. & Wasylikowa, K. Numerical analysis of charred seeds and fruits from an 8000 years old site at Nabta Playa, Western Desert, south Egypt. *Acta Palaeobot.***35**, 175–184 (1995).

63. Vartavan, C. de, Arakelyan, A. & Asensi Amorós, V. *Codex of Ancient Egyptian Plant remains*. (London: Sa, 2010).

64. Kletter, C. & Kriechbaum, M. *African traditional medicine: a dictionary of plant use and applications. With supplement: search system for diseases.African traditional medicine: a dictionary of plant use and applications. With supplement: search system for diseases.* (Medpharm, 2000).

65. Watt, J. M. & Breyer-brandwijk, M. G. *The Medicinal and Poisonous Plants of Southern and Eastern Africa being an Account of their Medicinal and other Uses, Chemical Composition, Pharmacological Effects and Toxicology in Man and Animal.The Medicinal and Poisonous Plants of Southern and Eastern Africa being an Account of their Medicinal and other Uses, Chemical Composition, Pharmacological Effects and Toxicology in Man and Animal.* (E. & S. Livingstone Ltd., 1962).

66. Fahmy, A. G., Kahlheber, S. & D'Andrea, A. C. Windows on the African Past: Current Approaches to African Archaeobotany. *Reports in African Archaeology* 242 (2011).

67. Attia, E. A. E., Marinova, E., Fahmy, A. G. & Baba, M. Archaeobotanical studies from hierakonpolis: Evidence for food processing during the predynastic period in Egypt. in *Plants and People in the African Past: Progress in African Archaeobotany* 76–89 (Springer International Publishing, 2018). doi:10.1007/978-3-319-89839-1_5.

68. Van Wyk, B.-E. A Review of African Medicinal and Aromatic Plants. in 19–60 (Springer, Dordrecht, 2017). doi:10.1007/978-94-024-1120-1_2.

69. Guasch-Jané, M. R., Ibern-Gómez, M., Andrés-Lacueva, C., Jáuregui, O. & Lamuela-Raventós, R. M. Liquid Chromatography with Mass Spectrometry in Tandem Mode Applied for the Identification of Wine Markers in Residues from Ancient Egyptian Vessels. *Anal. Chem.***76**, 1672–1677 (2004).

70. Cataldi, T. R. I. & Nardiello, D. Determination of free proline and monosaccharides in wine samples by high-performance anion-exchange chromatography with pulsed amperometric detection (HPAEC-PAD). *J. Agric. Food Chem.***51**, 3737–3742 (2003).

71. Dasenaki, M. E., Drakopoulou, S. K., Aalizadeh, R. & Thomaidis, N. S. Targeted and Untargeted Metabolomics as an Enhanced Tool for the Detection of Pomegranate Juice Adulteration. *Foods***8**, 212 (2019).

72. Kucharski, R. & Maleszka, R. Arginine kinase is highly expressed in the compound eye of the honey bee, Apis mellifera. *Gene***211**, 343–349 (1998).

73. Beye, M. The dice of fate: The csd gene and how its allelic composition regulates sexual development in the honey bee, Apis mellifera. *BioEssays* vol. 26 1131–1139 (2004).

74. Hendy, J. *et al.* A guide to ancient protein studies. *Nature Ecology and Evolution* vol. 2 791–799 (2018).

75. Tanasi, D. *et al.*^{1}H NMR,[1]H-[1]H 2D TOCSY and GC-MS analyses for the identification of olive oil in Early Bronze Age pottery from Castelluccio (Noto, Italy). *Anal. Methods* (2018) doi:10.1039/c8ay00420j.

76. Tanasi, D. *et al.* Paleoproteomic profiling of organic residues on prehistoric pottery from Malta. *Amino Acids***53**, 295–312 (2021).

77. Greco, E. *et al.* Proteomic Analyses on an Ancient Egyptian Cheese and Biomolecular Evidence of Brucellosis. *Anal. Chem.***90**, 9673–9676 (2018).

78. Gurdeep Singh, R. *et al.* Unipept 4.0: Functional Analysis of Metaproteome Data. *J. Proteome Res.***18**, 606–615 (2019).

79. Birarda, G. *et al.* Chemical analyses at micro and nano scale at SISSI-Bio beamline at Elettra-Sincrotrone Trieste. in *Biomedical Vibrational Spectroscopy 2022: Advances in Research and Industry* (ed. Huang, Z.) 31 (SPIE, 2022). doi:10.1117/12.2607751.

80. Zougman, A., Selby, P. J. & Banks, R. E. Suspension trapping (STrap) sample preparation method for bottom-up proteomics analysis. *Proteomics***14**, 1006–0 (2014).

81. HaileMariam, M. *et al.* S-Trap, an Ultrafast Sample-Preparation Approach for Shotgun Proteomics. *J. Proteome Res.***17**, 2917–2924 (2018).

82. Cox, J. *et al.* Accurate proteome-wide label-free quantification by delayed normalization and maximal peptide ratio extraction, termed MaxLFQ. *Mol. Cell. Proteomics***13**, 2513–26 (2014).

83. Valentini, A., Miquel, C., … M. N.-M. ecology & 2009, undefined. New perspectives in diet analysis based on DNA barcoding and parallel pyrosequencing: the trnL approach. *Wiley Online Libr.***9**, 51–60 (2009).

84. Pallavicini, A. & Florian, F. Plant metabarcoding analysis in a Ptolemaic Egyptian Bes-vase. *[Dataset]* (2024) doi:10.5281/ZENODO.7954932.

Table

Table 1. Summary and categorization of the substances found in the sample.

Nutraceutical substances	Medicinal substances	Psychotropic substances	Biological substances
Royal jelly	*Cleome* plant	*Peganum harmala*	Mucin-5B (oral or vaginal mucus)
Common wheat (traces)		*Nymphaea nouchali var. caerulea*	Lactotransferrin (breast milk)
Sesame seeds (traces)			Prolactin-inducible protein (breast milk)
Fruit yeast water (probably grapes)			Serum albumin (breast milk)
Pine derivatives			Hemoglobin subunit beta (human blood)
Licorice (traces)			Gamma-glutamylcyclotransferase (human blood)

Figures

Figure 1

a) Drinking vessel in shape of Bes head; El-Fayūm Oasis, Egypt; Ptolemaic-Roman period (4th century BCE - 3rd century CE), (courtesy of the Tampa Museum of Art, Florida). b) Bes mug from the Ghalioungui collection, 10.7 x 7.9 cm (Ghalioungui, G. Wagner 1974, Kaiser 2003, cat. no. 342). c) Bes mug inv. no. 14.415 from the Allard Pierson Museum, 11.5 x 9.3 cm (courtesy of the Allard Pierson Museum, Amsterdam; photo by Stephan van der Linden). d) Bes mug from El-Fayum, dimensions unknown (Kaufmann 1913; Kaiser 2003, cat. no. 343).
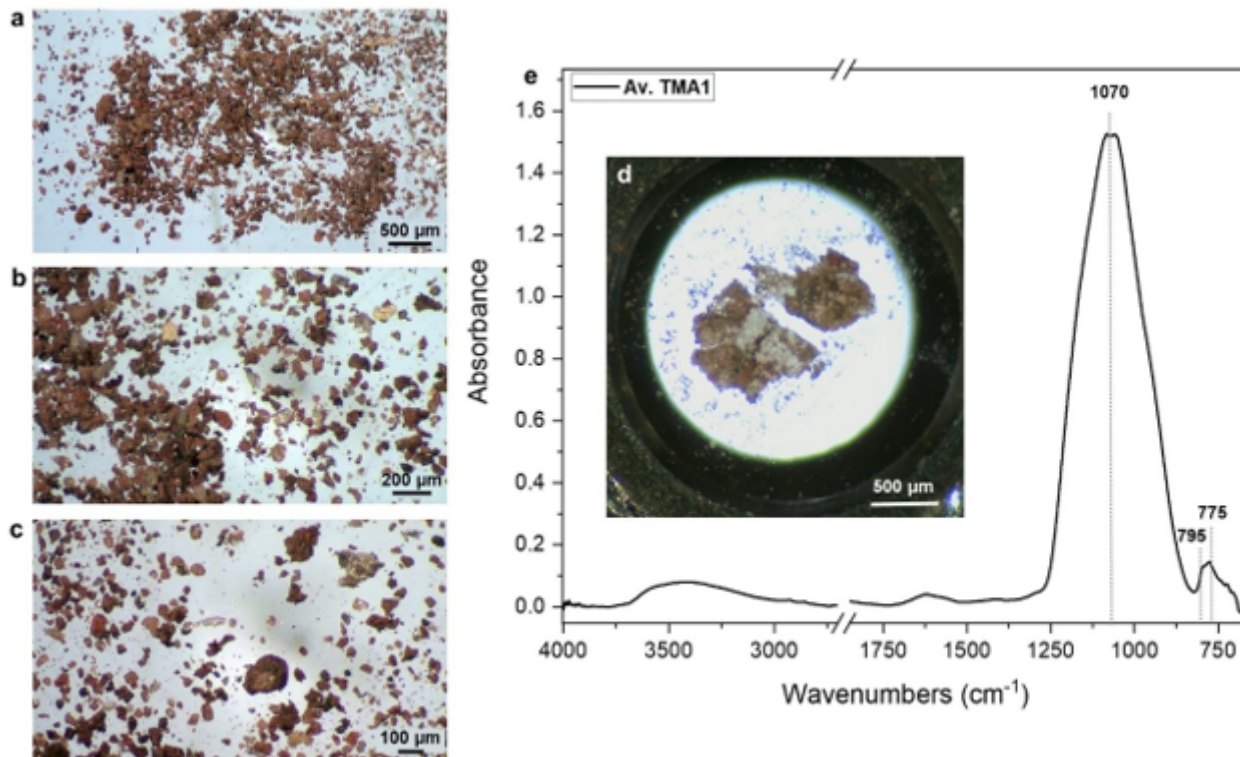
Figure 2

a-c) optical image of the sample collected from the Bes vessel at different magnifications. d) optical image of sample TMA1 flattened on half diamond compression cell. e) average spectrum of sample TMA1.
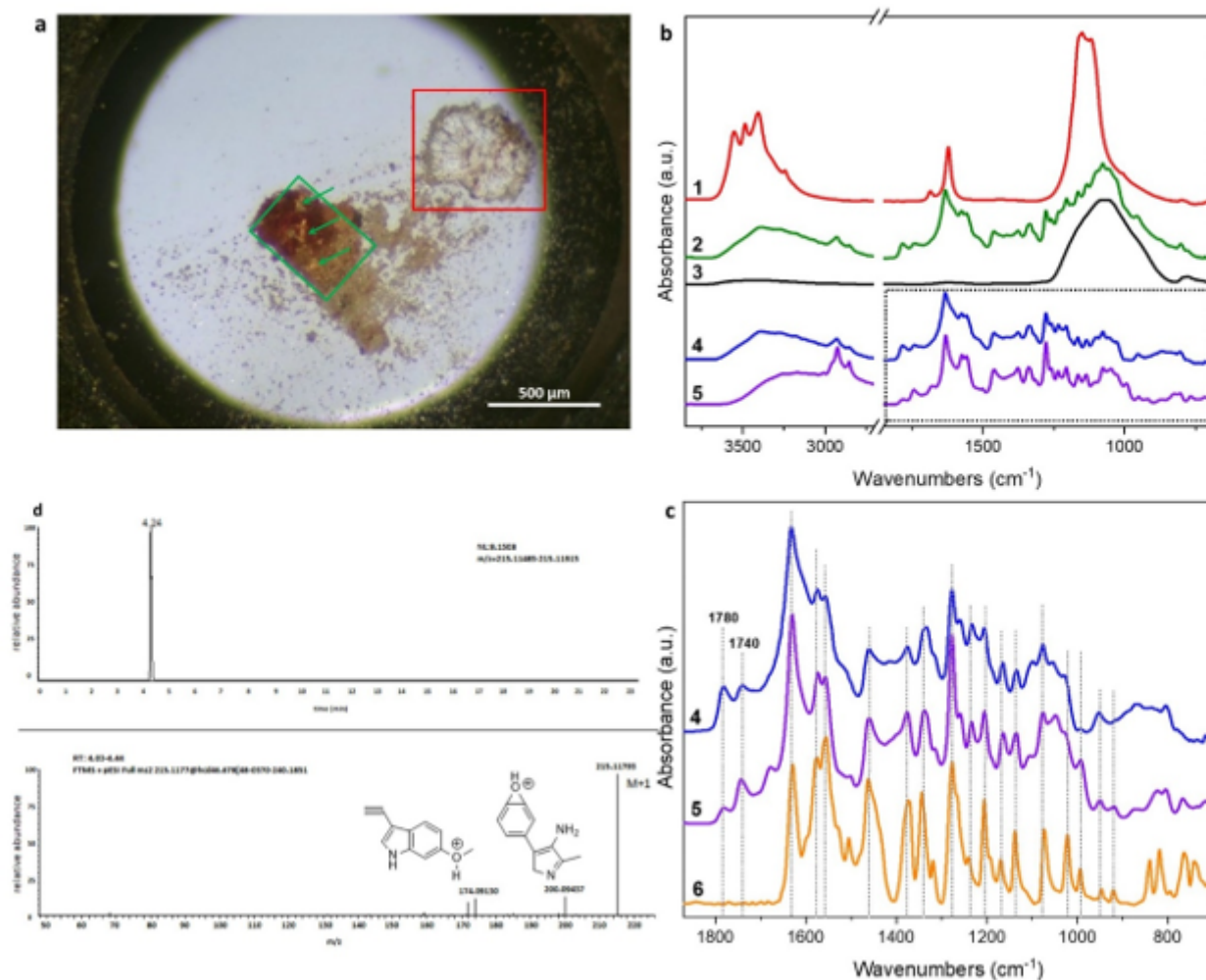
Figure 3

a) optical image of sample TMA2. b)1: average spectrum of the region in the red frame of panel a; 2: average spectrum of the region in the green frames in panel a; 3: average spectrum of sample TMA1; 4: subtraction spectrum obtained by subtracting 2-3; 5: Syrian rue seeds hydroalcoholic extract. c) HRMS spectrum and structure of harmaline d) Fingerprint region of spectrum 4 and 5 compared with a harmaline reference spectrum (6).
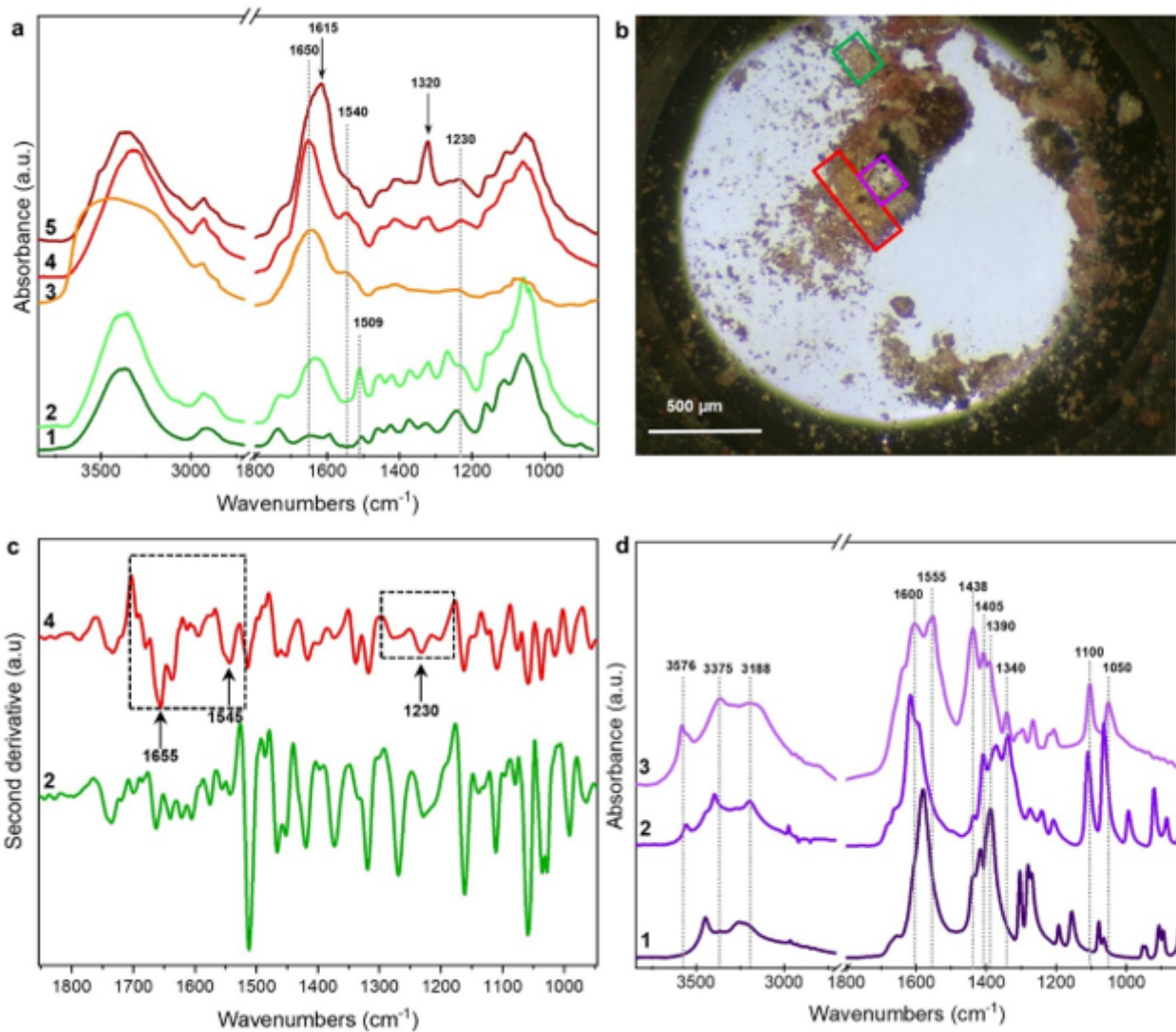
Figure 4

a) 1: reference spectrum of modern wood sample; 2: average spectrum of the region in the green frames in panel b; 3: reference spectrum of royal jelly; 4 and 5: average spectra collected in the area in the red frame of panel b; b) optical image of sample TMA3. c) second derivative spectra in the range 1900-900 cm^{-1} of spectra 2 and 4 in panel a. d) 1: reference spectrum of a sodium citrate; 2: reference spectrum of sodium tartrate; 3: average spectrum collected in the area in the purple frame of panel b.
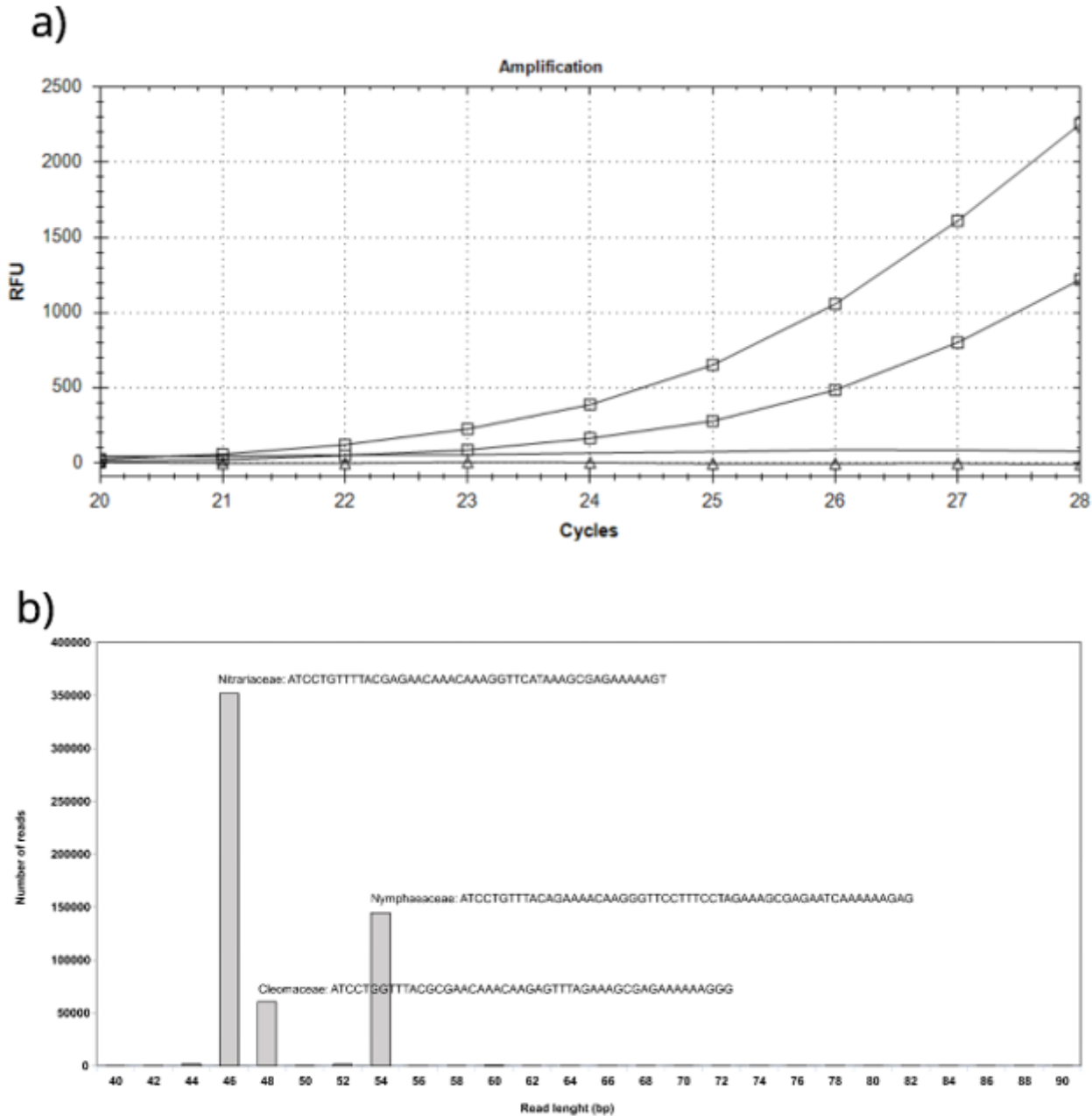
Figure 5

a) Plant DNA barcode amplification signal. Lines marked with square amplification of the tnrL intron system on DNA extracted, in duplicate, from the powder scraped from the BES-vase. Lines with triangle and continuous are respectively the amplification signal on mock extraction and control amplification reagents. b) Clustering of reads obtained from amplicon mass sequencing. Three main clusters of different lengths were unequivocally associated with the indicated plant families. On the y-axis the number of reads for each cluster.

Supplementary Files

This is a list of supplementary files associated with this preprint. Click to download.

- SupplementaryInformationANON.docx